'91 KACC 1991. 10. 22~24

Dynamic Characteristics of an LDPE Autoclave Reactor with Heat Transfer

Jinsuk Lee, Kil Sang Chang*, and Hyun-Ku Rhee

Department of Chemical Engineering, Seoul National University
* Central Research Center, Hanyang Chemical Corporation

ABSTRACT - A compact type LDPE autoclave reactor is analyzed with respect to the effects of the initiator feed concentration and the rate of heat transfer by employing the mixing-cell model with backflow. Singularity theory is applied for the single-cell model so that one can construct all the possible bifurcation diagrams. Since the single-cell model may not be adequate for the actual reactor, a two-cell model is also treated to predict the dynamic behavior of the reactor. As the rate of heat transfer increases, various multiplicity patterns and oscillatory motions are found. Apparently, the monomer conversion can be substantially increased with proper heat removal and initiator supplement scheme. For this, however, the complex dynamic features accompanied must be taken into consideration in the reactor design.

INTRODUCTION

After the LDPE was first synthesized by ICI(Imperial Chemical Industries) in the 1930's, various processes for the production of the LDPE have been proposed by many chemical companies. The processes, however, can be distingushed mainly by the reactor part and the other parts of the processes are almost alike. Two kinds of LDPE reactors, the tubular reactor and the autoclave reactor, are in use. The former shares the world-wide production of the LDPE by 55 %, and the latter by 45 %. While the behavior of the tubular reactor has been well examined by various authors[2,3,15], the characteristics of the autoclave reactor is left unexplored on the whole although a few pioneerig works[6,11,14] have been reported in the area of reactor simulation.

There are two different types of autoclaves: one is the slim reactor introduced and developed by ICI and the other is the compact type which was developed by Du Pont[7]. Both types are operated at 1000 ~ 3000 atm and 150 ~ 300 ℃. Fig. 1(a) shows a compact type reactor. This type of reactor has an L/D ratio of between 2 and 5, well-stirred reaction chamber, and the agitator motor located outside the reactor. The compact reactor does not lend itself for division into compartments due to its geometrical structure.

As autoclaves are characterized by smaller conversion than tubular reactors, attempts have been made to increase the conversion by removing some of the reaction heat with the aid of internal cooling device consisting of a liner with cooling coil for the passage of coolant[cf. Fig. 1(b)].

Here we shall present a detailed analysis of the steady state and dynamic behavior of a compact type LDPE autoclave reactor. In particular, the heat effect caused by the internal cooling tube on the reactor performance will be elucidated.

MODEL DEVELOPMENT

Although the LDPE polymerization reaction takes place at high pressure and temperature, the reaction is regarded to follow the conventional free radical mechanism. Elementary reactions considered in this study are initiation, propagation, termination, and chain transfer to monomer. The analysis of stability and dynamics does not depend on the polymer molecular weight distribution(MWD) since the moment equations have no feedback on the reactor dynamics. Although these equations are included in some calculations, the MWD results are not presented in this study but will be presented in the future work.

Due to its small L/D ratio the compact type reactor may be represented by the single-cell model or the two-cell model with backflow. For the two-cell model as shown schematically in Fig. 2, the mass balances of monomer, initiator, and total living polymers and the energy balance yield a set of eight ordinary differntial equations which can be put in dimensionless form as follows:

$$\mu\, dx_1/d\tau = \alpha + \beta x_2 - (\alpha+\beta)\, x_1 - \mu\, R_{x1} \quad (1)$$

$$\mu\, dy_1/d\tau = \alpha + \beta y_2 - (\alpha+\beta)\, y_1 - \mu\, R_{y1} \quad (2)$$

$$\mu\, dz_1/d\tau = \beta z_2 - (\alpha+\beta)\, z_1 - \mu\, R_{z1} \quad (3)$$

$$\mu\, dw_1/d\tau = \alpha + \beta w_2 - (\alpha+\beta)\, w_1 - \mu\, R_{w1} \quad (4)$$

for the cell 1 and

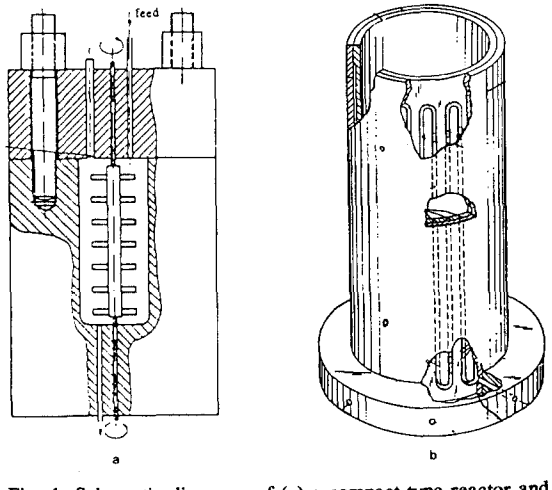

Fig. 1. Schematic diagrams of (a) a compact type reactor and (b) a reactor with internal cooling device[13].

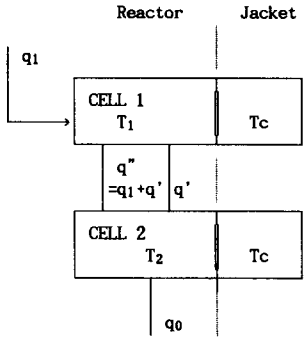

Fig. 2 Schematic diagram of the two-cell model for the compact type autoclave reactor.

$$(1-\mu)\ dx_2/d\tau = (1-\alpha) + (\alpha+\beta)x_1 - (1+\beta)\ x_2 - (1-\mu)\ R_{x2} \quad (5)$$
$$(1-\mu)\ dy_2/d\tau = (1-\alpha) + (\alpha+\beta)y_1 - (1+\beta)\ y_2 - (1-\mu)\ R_{y2} \quad (6)$$
$$(1-\mu)\ dz_2/d\tau = (\alpha+\beta)z_1 - (1+\beta)\ z_2 - (1-\mu)\ R_{z2} \quad (7)$$
$$(1-\mu)\ dw_2/d\tau = (1-\alpha) + (\alpha+\beta)w_1 - (1+\beta)\ w_2 - (1-\mu)\ R_{w2} \quad (8)$$

for the cell 2, where

$$R_{xj} = -\ Da_i\ x_j\ \exp(\gamma_d(w_j-1)/w_j) \quad (9)$$

$$R_{yj} = -\ 2f\phi Da_i\ x_j\ \exp(\gamma_d(w_j-1)/w_j) - Da_p\ y_j\ z_j\ \exp(\gamma_p\ (w_j-1)/w_j) - Da_{tm}\ y_j\ z_j\ \exp(\gamma_{tm}\ (w_j-1)/w_j) \quad (10)$$

$$R_{zj} = 2f\phi Da_i\ x_j\ \exp(\gamma_d\ (w_j-1)/w_j) - Da_t\ z_j^2\ \exp(\gamma_t\ (w_j-1)/w_j) \quad (11)$$

$$R_{wj} = B_p\ Da_p\ y_j\ z_j\ \exp(\gamma_p\ (w_j-1)/w_j) + B_t\ Da_t\ z_j^2\ \exp(\gamma_t\ (w_j-1)/w_j) - \delta(w_j-w_c) + \varphi \quad (12)$$

in which the subscript j on x, y, z or w denotes the cell number. The dimensionless groups used in the above equations are defined as

$x_j = I_j\ /I_f$ $\quad y_j = M_j\ /M_f$ $\quad z_j = G_j\ /M_f$

$w_j = T_j\ /T_f$ $\quad w_c = T_c\ /T_f$ $\quad \phi = I_f\ /M_f$

$\tau = t\ /\ \theta$ $\quad \varphi = P\theta/V_t\rho C_pT_f$ $\quad \delta = UA_t\theta/V_t\rho C_p$

$\gamma_d = E_d/RT_f$ $\quad \gamma_p = E_p/RT_f$ $\quad \gamma_t = E_t/RT_f$

$\gamma_{tm} = E_{tm}/RT_f$ $\quad \alpha = q_1\ /q_0$ $\quad \beta = q'\ /q_0$

$\mu = V_1\ /V_t = A_1\ /A_t$

$Da_i = k_{d0}\ \exp(-\gamma_d)\theta$ $\quad Da_p = k_{p0}\ M_f\ \exp(-\gamma_p)\theta$

$Da_t = k_{t0}\ M_f\ \exp(-\gamma_t)\theta$ $\quad Da_{tm} = k_{tm0}\ M_f\ \exp(-\gamma_{tm})\theta$

$B_p = (-\Delta H_p)M_f/\ \rho C_p\ T_f$ $\quad B_t = (-\Delta H_t)M_f\ /\ \rho C_p\ T_f$

where $\theta = V_t\ /q_0$

Thus x_j, y_j, and z_j represent the dimensionless concentrations of the initiator, monomer and total living polymer, respectively, in each cell and w_j and w_c stand for the dimensionless temperatures of the j-th cell and coolant, respectively. We also include the heat released by agitating the reaction mixture by the term φ. The correlation for the power consumption P is taken from Dickey[4]. Note that μ denotes the volume fraction of the first cell and the mean residence time θ is defined for the entire reactor system.

Table 1 The standard operating conditions for the LDPE autoclave reactor.

ITEMS	Numerical values
T_f, K	300
T_c, K	400
f	1
q_0, q_1, 1/sec	20
θ, sec	20
q', 1/sec	60
V_1, l	160
V_2, l	240
ρ, g/l	407.64
C_p, cal/g·K	0.583

The numerical data used for the simulation of compact type reactor are given in Table 1. The initiator feed concentration and the heat tranfer coefficient will be taken as the parameter.

In this study, the singularity theory[1,8], a sort of global analysis method, is applied to the single-cell model. For the two-cell model, however, one can only rely on the numerical method. To study the steady state, it is often convenient to examine the dependence of the solution upon distingushed parameter; i.e., the bifurcation parameter. The bifurcation theory[9,10] will be of great help for the comprehensive analysis of a nonlinear system. Here we use the software package "AUTO" written by Doedel[5] with which we can follow the entire steady state branch except for the isolated one. This program can also compute the loci of limit points dividing the multiplicity regions on the parameter plane and the loci of Hopf bifurcation points from which emerges the periodic solution branch.

RESULTS AND DISCUSSION

Equations (1) through (4) with $\alpha=1$, $\beta=0$, and $\mu=1$ give the equations for the single-cell model. These equations can be combined to give a single steady state equation for the temperature if the pseudo steady state assumption is introduced for living polymers and the minor terms are eliminated. With the dimensionless initiator, monomer and living polymer concentrations given by

$$x = 1/(1 + Da_i\ \exp(\gamma_d\ (w - 1)/w)) \quad (13)$$
$$y = 1/(1 + Da_p\ \exp(\gamma_p\ (w - 1)/w)\ z) \quad (14)$$
$$z = \sqrt{\frac{2\ f\ \phi\ Da_i\ x\ \exp(\gamma_d(w-1)/w)}{Da_t\ \exp(\gamma_t(w-1)/w)}} \quad (15)$$

respectively, the steady state equation for the dimensionless temperature may be rearranged to give

$$F(w,p) = 1 - w + B_p\,Da_p \exp(\gamma_p\,(w-1)/w)\; y\; z - \delta(w-w_c) = 0. \quad (16)$$

To obtain the bifurcation set and the bifurcation diagram, we must solve the equations for the hysteresis variety as well as for the isola variety; i.e.,

$$F(w,p) = \partial F/\partial w\,(w,p) = \partial^2 F/\partial w^2\,(w,p) = 0 \quad (17)$$

or

$$F(w,p) = \partial F/\partial w\,(w,p) = \partial F/\partial \lambda\,(w,p) = 0 \quad (18)$$

respectvely. The hysteresis and isola varieties are obtained by eliminating w and λ from Eq. (17) or Eq. (18), respectively. If we take the bifurcation parameter λ as the initiator feed concentration I_f, $\partial F/\partial\lambda$ always has a non-zero value, so the isola variety does not exist. Global classification of multiplicity and uniqueness region in the (δ,T_c)-plane is shown in Fig. 3. Thus, we have a unique steady state in region I and the S-shaped multiplicity in region II.

Comparing the result of the single-cell model with the numerical result from the two-cell model, we find that there is no qualitative difference between the two models except for a new hysteresis phenomenon appearing at the low level of the coolant temperature and a small kink observed near the adiabatic condition in the two-cell model. Since most of the commercial LDPE polymerization reactors are operated adiabatically, the S-shaped multiplicity pattern would be commonly encontered.

Operated under high pressure, LDPE autoclave reactor has a large wall thickness, so the heat removal efficiency is usually very poor. If the internal cooling device mentioned earlier could be used, it is naturally expected to obtain higher monomer conversion within the allowable temperature limit. In this case, however, various dynamic features are observed including the limit cycles and the foci which are not observed in the adiabatic systems.

Now we will analyze the structure of (δ,I_f)-parameter space with the coolant temperature fixed at T_c = 400 K. Fig. 4 shows the multiplicity regions of steady states and the locus of Hopf bifurcation(HB) point represented by the dashed line. The number of steady states increses or decreases by the number of two when a solid line is crossed over. The

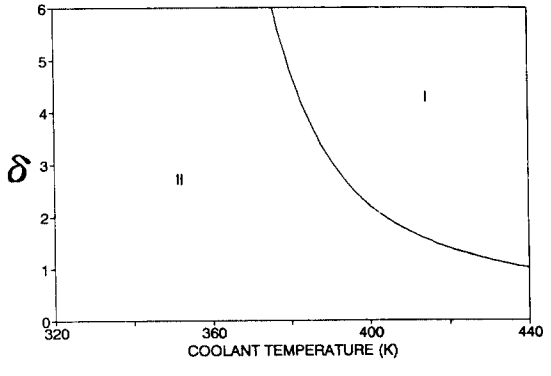

Fig. 3. Division of the the (δ,T_c)-plane into regions of different multiplicity patterns(based on the single-cell model).

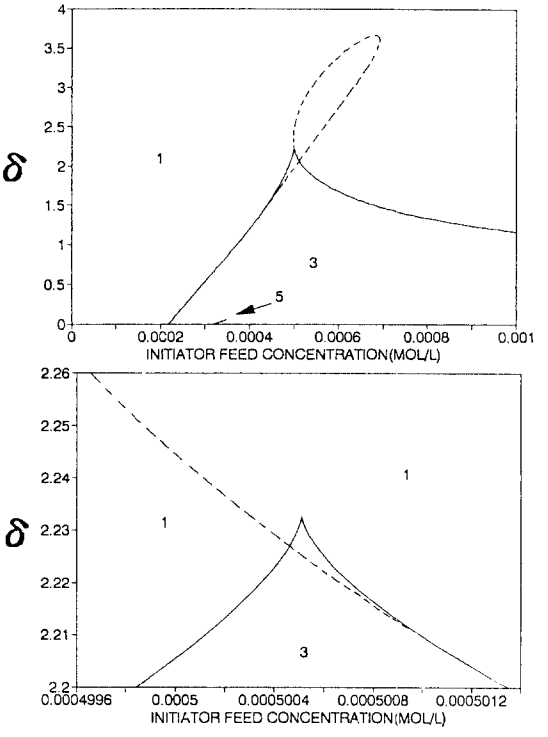

Fig. 4. Multiplicity regions of the steady states and the locus of the Hopf bifurcation point in the (δ,I_f)-plane.

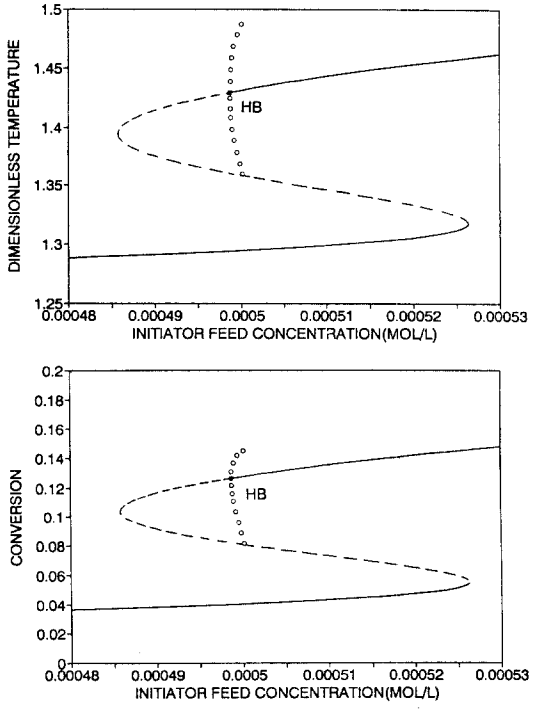

Fig. 5. Bifurcation diagram showing the steady state branch and the periodic solution branch when δ = 1.96.

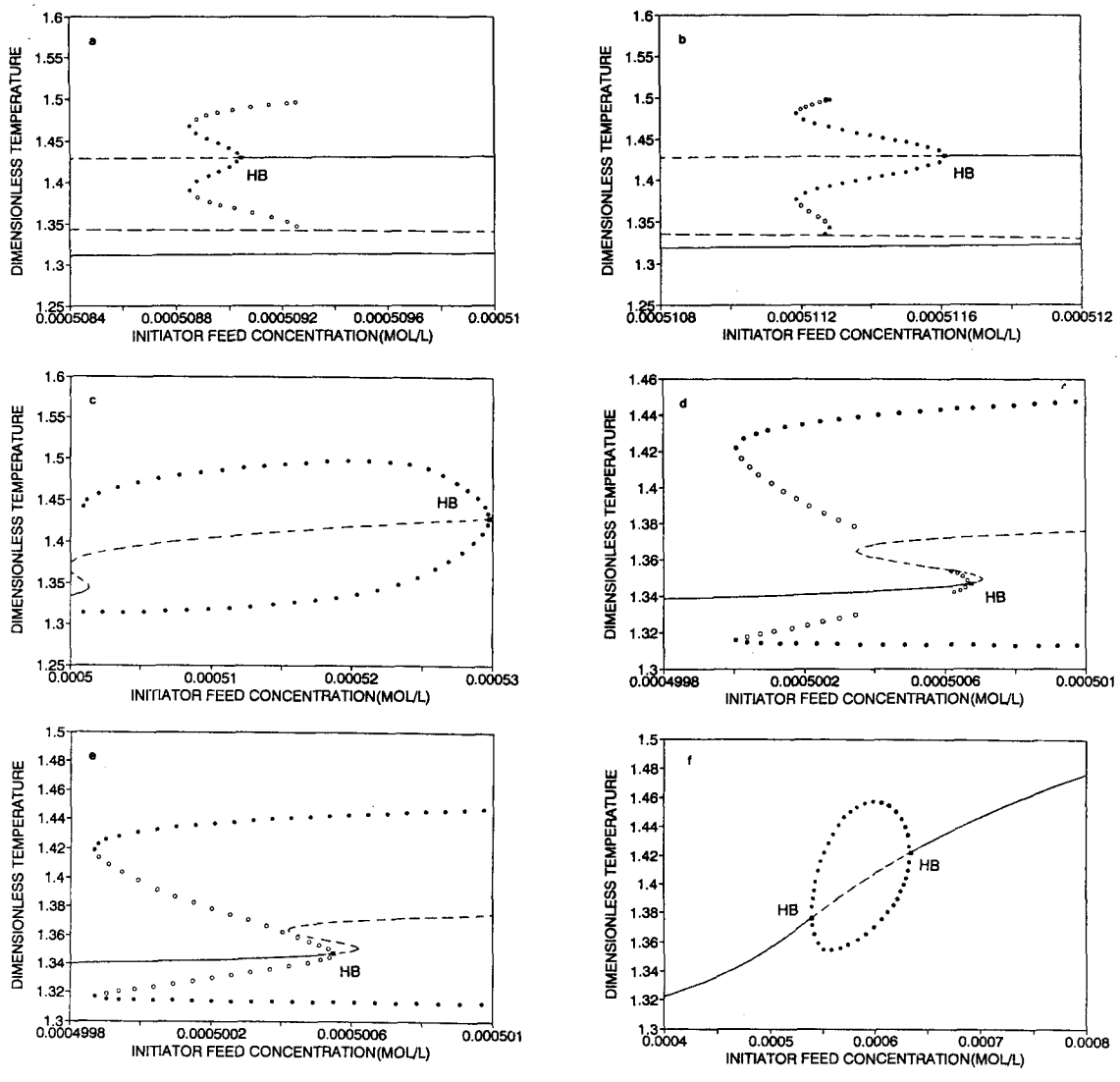

Fig. 6. Bifurcation diagram showing the steady state branch and the periodic solution branch when δ is equal to (a) 2.04, (b) 2.06, (c) 2.2, (d) 2.22, (e) 2.224, and (f) 3, respectively.

reactor dynamics could be quite complex having up to five steady states and the dynamic features may appear quite differently depending on the regions divided by solid or dashed lines.

It is observed from Fig. 4 that periodic oscillatory motions are to appear only for δ-values in the intermediate range. We do not expect to have in this system the isola of the periodic solution branch which was observed by Planeaux and Jensen[12].

First, fixing the value of δ at 1.96 and taking If as the bifurcation parameter, we construct the bifurcation diagram as shown in Fig. 5. One HB point is present on the upper steady state branch and the unstable periodic solution branch emanating from the subcritical HB point die away coalescing with the homoclinic orbit of an unstable saddle point. The steady state branch left of this HB point is an unstable focus and that on the right-hand side is a stable focus attractor. The bifurcation diagrams with δ-values lower than 1.96 show the similar features as Fig. 5.

The shape of the periodic branch changes as the heat transfer coefficient increases as shown in Fig. 6. Here the temperature is chosen as the state variable and other diagrams having the conversion of monomer or initiator and concentration of living polymer as the state variables exhibit the same qualitative features. Note that, in Fig. 6(a), the periodic solution branch emanating from the HB point starts out stable and then turns unstable at the turning point called the tangent bifurcation point, and the unstable periodic solution branch prevails until it dies away.

When the heat transfer coefficient increases to δ = 2.06 in Fig. 6(b), the periodic solution branch undergoes a couple of tangent bifurcations and a homoclinic explosion.

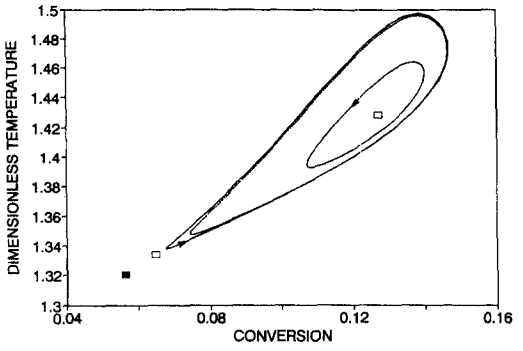

Fig. 7. Phase plane plot of the limit cycles when $\delta = 2.06$ and $I_f = 5.1128 \times 10^{-4}$ mol/l.

So we expect two stable limit cycles and one unstable limit cycle. One may note that an unstable limit cycle acts as a boundary of neighboring attractors like an unstable saddle point. Typical stable and unstable limit cycles for $\delta = 2.06$ are shown in Fig. 7. The three limit cycles in Fig. 7 have different periods and different amplitudes.

In the case of $\delta = 2.2$, the periodic solution is now fully stable and terminates at a saddle loop as one can see in Fig. 6(c). In most cases the homoclinic explosion is well visualized on a bifurcation diagram; i.e., the connection to a saddle point can be seen by the maximum or the minimum amplitude of a periodic solution branch. But the situation is not so in Fig. 6(c) and this can be better clarified with the help of a dynamic simulation close

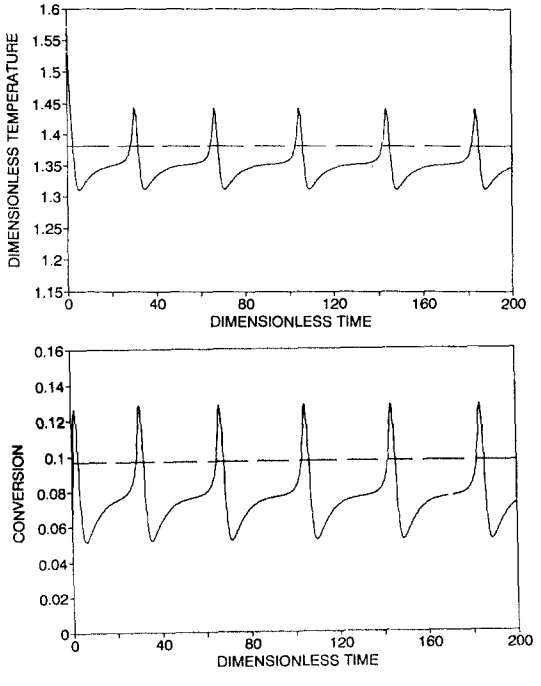

Fig. 8. Transient behavior of the temperature and the conversion near a homoclinic orbit when $\delta = 2.2$ and $I_f = 5.008910 \times 10^{-4}$ mol/l.

to a homoclinic orbit as shown in Fig. 8. The dashed lines represent the temperature and the conversion at the correseponding unstable steady state which is a saddle point. The period of oscillation in this case is about 40 times the reactor mean residence time.

In the bifurcation diagram of Fig. 6(d) for which $\delta = 2.22$, we have two HB points and also two homoclinic explosions by the periodic solution branch from each HB point. Hence, we expect that there exist a double zero dgeneracy between $\delta = 2.2$ and 2.22 as one may notice from Fig. 4 which occurs when an HB point and a limit point coincide. If δ increases a little further to 2.224, two periodic solution branches appeared in Fig. 6(d) coalesce with each other, or the two HB points are linked by a periodic solution branch which has one turning point. This is presented in Fig. 6(e).

If δ is increased up to 3, we have a unique steady state over the whole range of the bifurcation parameter and a unique periodic solution branch links two HB points as depicted in Fig. 6(f). When δ has a value larger than 3.669414, there is no HB point on the steady state branch. At first we expected to have an isola of periodic solution as was observed by Planeaux and Jensen[12], but in this system the periodic oscillatory behavior simply fades away as δ crosses over the value of 3.669414.

CONCLUSION

Mixing-cell model with back flow and heat transfer from jacket side appears to be adequate to predict the dynamic behavior of the compact type autoclave reactor for LDPE polymerization. A bifurcation analysis of the model with the initiator feed concentration as the bifurcation parameter shows rather complex dynamic features including periodic oscillatory motion.

As the rate of heat removal increases, one or more Hopf bifurcation points are present and the periodic solution branch takes different patterns to give a variety of oscillatory motions while the steady state multiplicity feature becomes simpified. With higher rates of heat transfer, however, the Hopf bifurcation points tend to disappear.

Since the dynamic features are sensitive to small changes in some parameters, a rigorous control policy seems essential in start-up or even in steady state operation so as not to escape the stable attraction regions. In particular, one may desire to avoid the region of limit cycle attractors to maintain uniform properties of the polymer product.

With sufficient initiator supplement, the monomer conversion could be substantially enhanced while the temperature runaway phenomenon accompanied may be effectively suppressed by installing a proper heat transfer equipment. For this, however, one should proceed with special care because the properties of the polymer product could be significantly affected.

NOTATION

C_P : heat capacity (cal/g·K)
E : activation energy (cal/mol)
f : initiator efficiency
G : total concentration of living polymers (mol/l)
$(-\Delta H)$: heat of reaction (cal/mol)
I : concentration of initiator (mol/l)
k : reaction rate constant : sec^{-1} for initiation, or l/mol·sec for propagation, termination, and chain transfer
M : concentration of monomer (mol/l)
P : power consumption by agitation (cal/sec)
q, q' : flow rates (l/sec)
R : gas constant (1.987 cal/mol·K) or dimensionless reaction rate
T : temperature (K)
t : time (sec)
V : reactor volume (l)

Greek letters :
$\gamma = E/RT_f$: dimensionless activation energy
λ : typical bifurcation parameter
ρ : density (g/l)
$\tau = q_0 t/V_t$: dimensionless time
$\theta = V_t/q_0$: mean residence time(sec)

Subscripts :
c : coolant
d : decomposition of initiator
f : feed
i : initiation
j : cell number
m : monomer
p : propagation or polymer
t : termination or total
tm : chain transfer to monomer

REFERENCES

[1] V.Balkotaiiah and D.Luss, "Global analysis of the multiplicity features of multi-reaction lumped-parameter systems," *Chem. Eng. Sci.*, 39, 865(1984).

[2] A.B.Brandolin, N.J.Capiati, J.N.Farber and E.M. Valles,"Mathematical model for high pressure tubular reactor for ethylene polymerization," *Ind. Eng. Chem. Res.*, 27, 784(1988).

[3] C.H.Chen, J.G.Venmeychuk, J.A.Howell and P.Ehrlich "Computer model for tubular high-pressure poly-ethylene reactors," *AIChE J.*, 22, 463(1976).

[4] D.S.Dickey,"Program chooses agitator,"*Chem. Eng. J.*, 9, 73(1984).

[5] E.J.Doedel and R.F.Heinemann,"Numerical computation of periodic solution branches and oscillatory dynamics of the stirred tank reactor with A→B→C reactions," *Chem. Eng. Sci.*, 38, 1493(1983).

[6] G.Donati, M.Gramondo, E.Langianni and L. Marini, "Low density polyethylene in vessel reactors ," *Ing. Chim. Ital.*, 17, 88(1981).

[7] A.M.Gemassmer, "The autoclave process for high-pressure polymerization of ethylene," *High Temperatures High Pressures*, 9, 507(1977).

[8] M.Golubitsky and D.G.Schaeffer, *Singularities and groups in bifurcation theory*, Vol. 1, Springer-Verlag, New York, 1984.

[9] G.Ioose and D.D.Joseph, *Elementary stability and bifurcation theory*, Springer-Verlag, New York, 1976.

[10] M.Kubicek and M.Marek, *Computational methods in bifurcation theory and dissipative structures*, Springer-Verlag, New York, 1983.

[11] I.Marini and C.Georgakis, "Low-density polyethylene vessel reactors," *AIChE J.*, 30, 401(1984).

[12] J.B.Planeaux and K.F.Jensen, "Bifurcation phenomena in CSTR dynamics: A system with extraneous thermal capacitance," *Chem. Eng. Sci.*, 41, 1497(1986).

[13] M.E.Pruitt and J.B.Lovett, "Polymerization of ethylene in stirred autoclave with cooled inner wall," United States Patent: 3,963,690(1976).

[14] J.S.Shastry and L.T.Fan, "Stability analysis in polymerization reactor system," *Chem. Eng. J.*, 6, 129(1973).

[15] B.J.Yoon and H.-K.Rhee, "A study of the high pressure polyethylene tubular reactor," *Chem. Eng. Commun.*, 34, 253(1985).